# Late Wolstonian and Ipswichian (MIS 6/5e) sediment fill in a limestone sinkhole, Askham Fell, northern England

Paul A. Carling[1*], David J.A. Evans[2], Mahmoud Abbas[3], Xianjiao Ou[4], Zhongping Lai[3]

[1]Geography & Environmental Science, University of Southampton, Southampton, UK

[2]Department of Geography, Durham University, Durham, UK

[3]Institute of Marine Sciences, Guangdong Provincial Key Laboratory of Marine Disaster Prediction and Prevention, Shantou University, Shantou, 515063, China

[4]School of Geography and Tourism, Jiaying University, Meixhou, 514015, China

[*]Corresponding author

**Abstract**

In 2019 a sinkhole (doline) occurred in Late Devensian till above fissured limestone in northern England. Most sediment plugging the fissure was evacuated down into a karstic drainage system. The residual sedimentary fill comprises three main lithofacies, dated using optically stimulated luminescence to between 170.7ka ± 40.0ka and 56.1 ± 13.5ka. The earliest date demonstrates fissures occurred in the limestone pavement at the time of Marine Isotope Stage 6, or shortly thereafter. The fissure filled with fine sand and silt due to surface runoff and aeolian processes most likely at the Marine Isotope Stage (MIS) 6 to MIS 5e transition after Wolstonian glacial ice had retreated. The deposits then collapsed into the karst system. Further fine sand and silt deposition occurred during MIS 3; this deposit filled the central cavity surrounded by residual MIS 6/5e deposits. The sequence was capped by till as Late Devensian (MIS 2) ice transgressed the area. Solution fissures in the karst surfaces of northern England may pre-date the Late Devensian glaciation. Moreover, fissures are repositories of pre-Devensian sediment deposits which survived the Late Devensian glaciation and the Ipswichian interglacial. Such sites should provide information on the nature and timing of pre-Devensian glacial-interglacial events and shed light on basal ice conditions and glaciokarst drainage behaviour.

Key words: Limestone sinkhole; karst; glaciation; Wolstonian; Ipswichian

## Introduction

Glaciokarst landscapes have been widely reported globally (Veress et al. 2019) and are prominent across the limestone terrains of northern England (Waltham & Lowe, 2013), where karst surfaces have been influenced, to a greater or lesser extent, by the action of glacial ice and meltwater primarily during the Dimlington Stadial of the Devensian glaciation (~28-15 ka; Rose, 1985; Scourse *et al.*, 2009; Chiverrell & Thomas, 2010; Davies *et al.*, 2019). As well as bare limestone landforms such as pavements, thin layers of drift (glacigenic diamicton/till or loess lenses in hollows) are widely distributed over the karst surfaces (Waltham, 2013). Drift often overlies and plugs solution-widened vertical fissures and cone-shaped depressions in the limestone. Collapse of the drift down into fissure systems, due to gravity and surface water percolation, also results in conical depressions in the drift where the infill has collapsed into the basal fissure network (Evans & Young, 2022). In the UK context, Goldie (1996) proposed the term 'runnel hole' for any smaller solution-widened fissure and larger cone-shaped depressions (whether formed in bedrock or drift) individually are essentially dolines (Jennings, 1975; Ford & Williams, 1989; Veress, 2019) but also are termed 'pothole', 'swallet', ‘shakehole’ ‘or sinkhole’ when referring to smaller scale features. Although Sweeting (1972) and Waltham (2013) adopted the term ‘shakehole’ for features developed in glacial deposits, the term ‘sinkhole’ is probably better understood worldwide and so is used herein. Where doline formation predates recent glaciations, they have the potential to be valuable stratigraphic repositories for Quaternary environmental changes (e.g. Ford & Stanton, 1968; West et al. 2014).

The heights and diameters of these sinkholes are delimited by the drift thickness with an extension of variable depth into wider limestone conical depressions; the basal fissures may be open, or sediment choked. The fissures may terminate at relatively shallow depths or connect to deeper karstic cavern systems. Little is known of the nature and age of diamicton often found within sinkholes and the timing of solution widening of fissures and hollows remains debatable. For example, Waltham (2013) believed the process of fissure widening pre-dates the Devensian, with sinkhole fill being of Devensian age. Clayton (1981) suggested that deepening of hollows beneath the drift may have occurred by subsoil dissolution during interglacial periods which clearly associates both fissure development and placement of some of the infill within a pre-Devensian period of time, for example the Ipswichian (Eemian) interglacial stage. Vincent (1995) and Goldie (1996) speculated that Devensian ice may not have been able to erode sinkhole fill, so some fill might be pre-Devensian.

The appearance in 2019 of a new sinkhole in drift above limestone bedrock on Askham Fell in Northern England (Fig. 1) provided an opportunity to describe and date the sediment fill. The purpose of the exercise was to: i) enhance understanding of the sedimentary fill found within sinkholes; ii) derive timescales for the karst processes associated with sinkhole formation; and iii) shed light on sinkhole formation processes. Better understanding of this specific sinkhole should provide guidance as to how sinkholes have evolved more generally within glaciokarst landscapes.


*Figure 1: Location of the Askham Fell sinkhole (red dot). Location of the study area within the UK is shown in the inset. Base map from Ordnance Survey, https://digimap.edina.ac.uk.*

**Environmental context of the Askham Fell sinkhole**

Askham Fell is underlain by Carboniferous rocks, primarily the Shap Village Limestone Formation, which varies in thickness between 40m and 150m (McCormac, 2003). The thin beds consist of limestone/dolostone with siltstone interbeds. The planar nature of the land surface reflects the fact that the limestone exposure is a smoothed pavement. Circular to ovoid funnel-shaped sinkholes up to 30m in diameter and less than 10m deep, are frequent across the areas known as Moor Divock and Tarn Moor (Fig. 1). They are primarily developed in thin till, but some exhibit open limestone shafts at their bases, whilst others are plugged by diamicton, although freely draining. A few sinkholes contain permanent small ponds due to blockage of the basal drainage points.

The sinkholes trace-out a meandering line that snakes from a group called Pulpit Holes in the NW, through Wofa (var. Wolfa) Holes to Dewpot Holes in the SE (Fig. 1); clearly following the curvature of the Shap Village Limestone outcrop. Overall, the presence of sinkholes indicates the presence of a rudimentary sub-surface karstic drainage system, linking solution-opened fissures, joints and bedding planes (Waltham *et al*., 2005), today draining precipitation concentrating in the sinkholes. The area was glaciated as recorded by a Late Devensian till, which occurs patchily as a thin discontinuous cover (McCormac, 2003), less than 1m thick, above a thin patchy weathered regolith that lies directly on the basement limestone pavement. Limited augering (excluding sinkholes; Clare & Wilkinson, 2006) on Tarn Moor demonstrated the discontinuous nature of the till; *i.e.*, up to 0.63m thickness of peat was recorded above a thin mineral regolith on drier areas and thin sphagnum peat above organic-rich clays (< 0.55m thick) deposited in wetter hollows.

The described section (N: 54.588596; W: 2.781580), at 315m above sea level, appeared in 2019 on the western slope of a small eminence called "The Rigg", when the diamicton at the ground surface collapsed to form a funnel-shaped depression, exposing open fissures in the limestone at depth. The collapsed sediment was washed away down the karstic drainage system below. This type of sinkhole has been termed a 'dropout' (Waltham & Fookes, 2003; Waltham *et al*., 2005) where a dissolution enhanced fissure had been filled by diamicton to lose surface expression, only to be revealed later by the collapse mechanism. Google Earth images from 2018 show no surface expression of the sinkhole (Fig. 2). Later collapse may have been due to progressively enlarged dissolution pockets in the limestone, causing structural failure of the limestone bedding and allowing the sedimentary infill to disappear deeply within the system to leave a 10m diameter surface scar (Fig. 3). Alternatively, a sedimentary blockage lying above a void at depth may have lost mechanical competence. In either case, the basal limestone bedding in the exposed portion of the sinkhole remained intact and, in June 2021, seepage water was observed to drain into limestone fissures and cavities at the base of the hollow.


*Fig. 2: Vertical aerial view of the sinkhole location in 2018 and in 2019. Note the absence of surface expression of an underlying sinkhole in 2018 (blue arrow). Map data ©2019 Google.*


*Figure 3: Sinkhole in 2020*

**Methods**

The exposed sedimentary section within the sinkhole was cleared of debris using a spade and then trowelled to provide a clean full section. The basic stratigraphy was sketched, unit thicknesses measured and visual details such as colour and texture recorded. Samples were taken for grain-size analysis and basic chemical determinations. A Malvern Mastersizer was used to determine the grain-size distributions of each sample. Loss-on-ignition was used to determine the organic, organic carbon, carbonate content and calcium carbonate contents (Hoogsteen *et al*., 2018).

Three samples were taken for optically stimulated luminescence (OSL) dating using 5 cm diameter and 10 cm long aluminium tubes driven horizontally into the section within three distinct sandy stratigraphic units (see Results). As the sandy units are relatively thin, an OSL sample was taken from the centre of each three layers to date the median timing of the deposition of the layer. Samples were dated using a single aliquot regenerative dose (SAR) protocol (Murray & Wintle, 2000) applied to the single grains at Jiaying University, Meizhou, China. Further sample details and the full method for the laboratory determination of OSL dates are provided within Supplementary Information.

**Results**

The stratigraphy of the sedimentary fill within the sinkhole is described below and the dates of the sedimentary units are reported, following which, a model for the evolution of the sedimentary fill is outlined. The implications of these results with respect to the environment of deposition and the timing of development of the solution fissures in the regional basal limestone are considered within the Discussion.

*Stratigraphy*

Summary Description of Sedimentary Section

The collapse revealed a 2.65m high section (Fig. 4A), the base of which comprises poorly exposed, *in situ* and horizontally thinly bedded (typically 10 to 20 cm thick beds) and highly fissured limestone. The basal limestone is weathered, and joints and bedding planes have been subject to dissolution by water erosion, but visible horizontal fissures are infilled by silt and sand, in places displaying a black colouration; iron-manganese concentration, causing black discoloration of sediment, is common in Pennine karst cave networks (Murphy, 1999). As these lower fissure deposits have uncertain stratigraphic context and the associated erosion and deposition could have occurred on multiple occasions, thereby lacking temporal constraint, they were not sampled. Within the overlying sediments there is substantial evidence of soft-sediment deformation due to slumping. These mass movements include microfaults constraining intact blocks of failed sediment at various levels and localised fold disruption of bedding. The issue of repeated collapse of strata is considered within the Results. Nevertheless, the cleaned exposure within the sinkhole facilitated a description of five distinct stratigraphic units or lithofacies (Fig. 4B), with unit LF 1 inset (see below).

Below the sedimentary lithofacies lies intact limestone (LF 0), which is *c*.0.5m thick and with fissures infilled with an upper yellow sand overlying a darker sandy basal fill. Moist and dark compacted sandy silt coats the limestone surfaces (including vertical surfaces), often infilling fissures completely. LF 0 is not described further (and was not sampled) but extends to depths which could not be examined.

LF 1 is a distinct yellow fine sand, up to 0.70 m thick in places and intruding into the top of the limestone. It is horizontally laminated (1 – 10 mm thickness) and exhibits occasional thin dark bands, indicative of chemical alteration. LF 1 was sampled for OSL dating.

LF 2 is a dark brown fine sand, exhibiting thin (mm thick) horizontal layering (lamination) that is locally disrupted by soft sediment deformation structures. It is 0.20 m thick and has sharp but gradational lower contact with LF 1 and a loaded deformed upper contact with LF 3. The dark colour may represent chemical alteration. LF 2 was sampled for OSL dating.

LF 3 is a 0.25 m thick, predominantly horizontally bedded/laminated, beige fine sand and displays characteristics similar to those of underlying LF 2 as well as some intrabeds of intact LF 2. Its upper few centimetres displays the characteristics of a mélange comprising deformed sand laminations together with some clasts derived from the overlying LF 4. An organic-rich vertical fissure extends through LF 3 but does not extend into the lithofacies above or below and is likely a root cast. LF 3 was sampled for OSL dating.

LF 4 is a massive, clast-rich, matrix-supported diamicton with a compact and highly fissile structure (Dmm(f)). This unit is 0.50 m thick in outcrop but continues a further 0.50 m above the sinkhole sides as an eroding surrounding slope. A clast macrofabric from the centre of the lithofacies reveals a relatively strong south-southeasterly orientation with an S1 eigenvalue of 0.56 (Fig. 5).

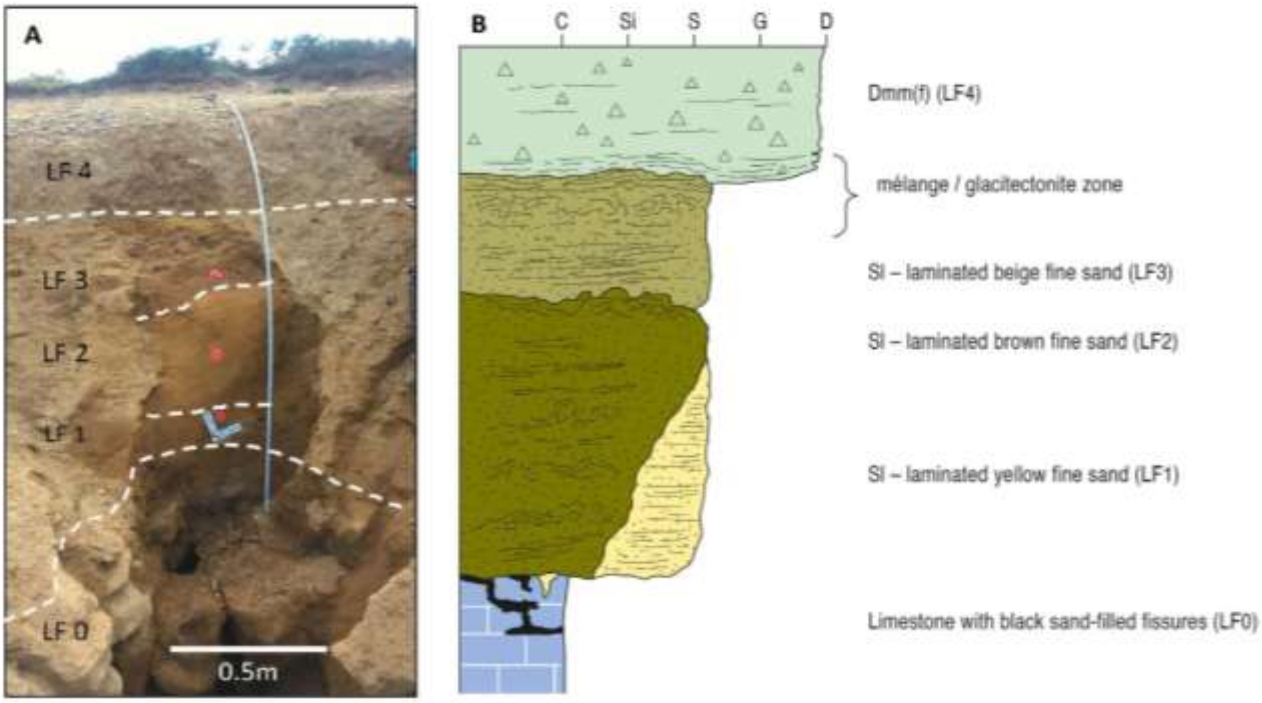


*Figure 4: A) View of cleaned section showing the location of lithological units LF 0 to LF 4 and the red tube OSL samples (unlabelled) from base to top: LF 1, LF 2 and LF 3; B) Stratigraphic column representing the cleaned section shown in panel A. Unit LF 1 is inset into the base of unit LF2, as explained in the Results.*

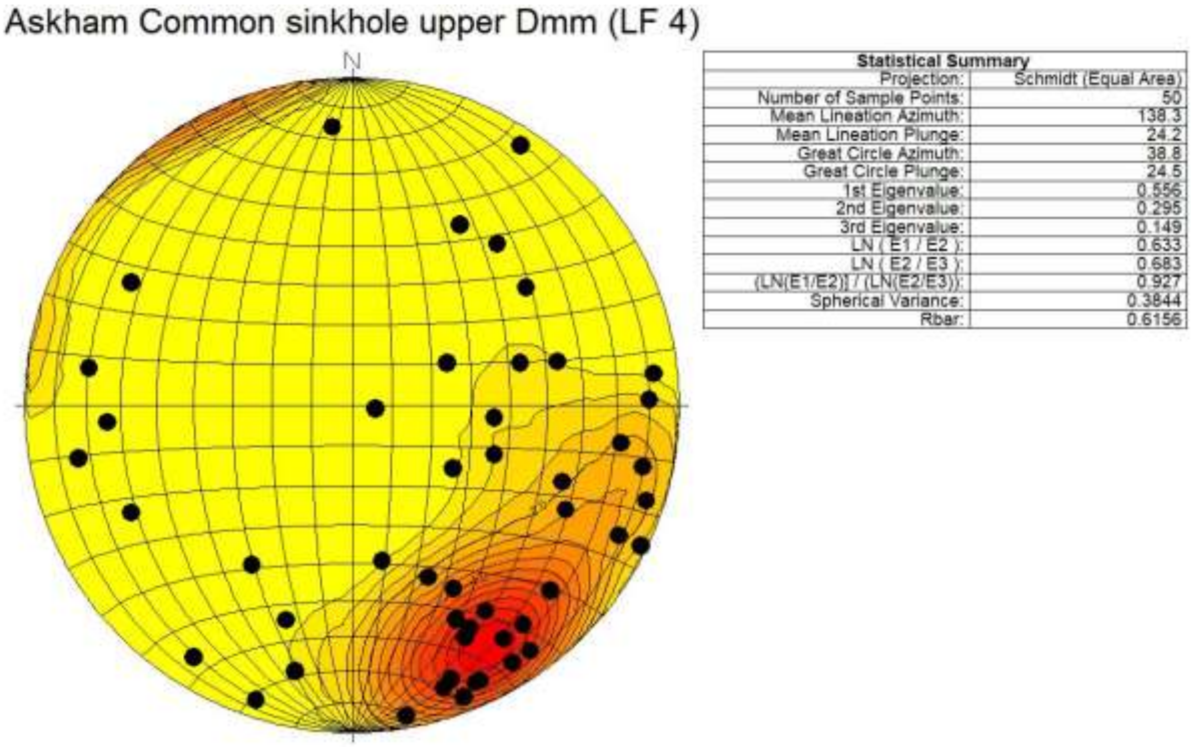

*Fig. 5: A clast macrofabric from the centre of the lithofacies LF 4 reveals a strong south-southeasterly orientation with an S1 eigenvalue of 0.56.*

Description and Interpretation of lithofacies

The basal limestone (LF 0) represents the heavily weathered surface layer of the Shap Village Limestone Formation, which has been subject to dissolution processes, opening both vertical joints and horizontal bedding planes over a substantial time period. At times, prior to the Dimlington Stadial, a limestone surface will have been exposed sub-aerially, exhibiting a thin soil, typical of that developed on limestone terrain. However, glaciation has removed any evidence of palaeosols. The presence of yellow sand (LF 1) filling the conduits at depth is consistent with continued downward percolation of drainage water through the sediment fill. In contrast, the black (unsampled) sandy fill, which tends to occur cemented to open limestone conduit surfaces at greater depths, represents a sand deposit that has been subject to a greater degree of diagenetic alteration, in contrast to the yellow sand. As noted above, the dark colour may represent iron-manganese precipitations, although this issue was not pursued.

Due to their similarity, LFs 1, 2 and 3 are presented here together. The organic content of the fill is modest throughout the deposits due to aerobic digestion, likely due to the sandy sediment being well-aerated and well-drained. Similarly, the calcium content is low in all cases (Table 1). The grain-size distributions for LFs 1-3 are similar, most likely reflecting similar depositional processes (Fig. 6). The samples are strongly bimodal. A coarser sandy-distribution ranges between 66.9µm and 454µm, whilst a finer distribution ranges between 0.0597µm and 45.6µm. The narrowly distributed coarser grain-size range of fine to medium sand represents in-wash of local surface-derived sediments by surface water drainage. The broad silt distributions are interpreted as a wind-blown component derived from abrasion and selective entrainment of surface deposited sediment within the general vicinity and then trapped in the sinkhole. Notably, two of the grain-size distributions exhibit a distinct grain-size ‘gap’ with no particles in the range between 45.6µm to 66.9µm, whilst the third sample exhibits a local minimum in the same range. Loess is usually finer than 50 µm, so the aeolian silty sediment can be interpreted as a loess with an extended fine clay tail. This aeolian sediment was deposited as an intimate admixture to the coarse in-wash, as the difference in the grain-size distributions is not evident stratigraphically.

The surface diamicton (LF 4) is rich in local limestone fragments. As the diamicton is compact and fissile, contains a basal mélange zone representative of a shear zone glacitectonite, and displays a distinct and relatively strong macrofabric orientated towards the south-southeast (Fig. 5), it is interpreted as a subglacial till emplaced by north-northeasterly flowing glacier ice (see protocols in Evans, 2018). This ice flow direction corresponds to the Dimlington Stadial LT6 phase of Livingstone *et al*. (2008; 2012), which represents the last predominant ice flow direction in the area at the close of the Late Glacial Maximum (LGM), when strong ice streaming was directed northwards down the Eden Valley towards the Solway Lowlands.

Table 1: Basic chemistry of the sediment samples

| Sample # | Organic content (%) | Organic carbon (%) | CO2 content (%) | Carbonate content (%) | Calcium carbonate content (%) |
|---|---|---|---|---|---|
| LF 1 | 0.52 | 0.21 | 0.25 | 0.34 | 0.57 |
| LF 2 | 1.04 | 0.42 | 0.63 | 0.86 | 1.44 |
| LF 3 | 1.53 | 0.61 | 0.90 | 1.23 | 2.05 |

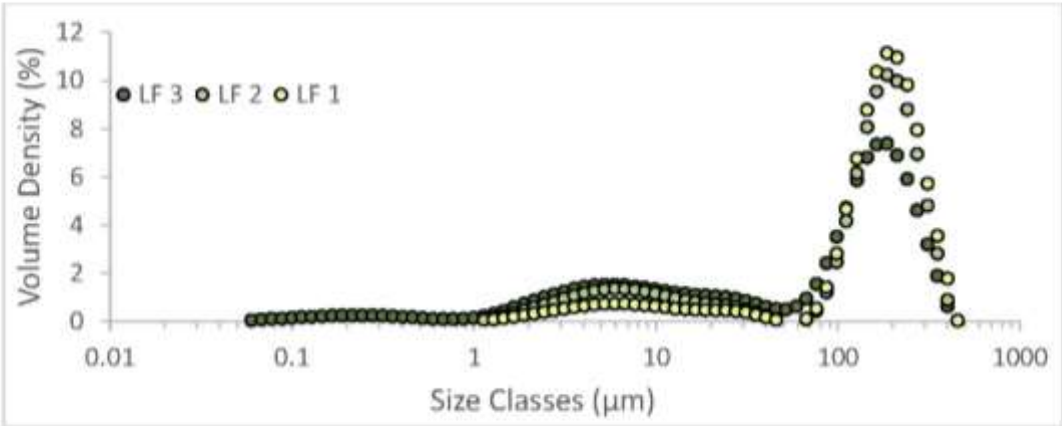


*Figure 6: Grain-size distributions for the infill. Note the grain-size 'gap' at 50 to 60µm that characterizes two samples. The gap separates two depositional components representing differing process domains. Each curve is the average for six determinations.*

*The Age of the Sedimentary Deposits*

Optically stimulated luminescence (OSL) dating was achieved using SAR protocol (Murray & Wintle, 2000) applied to quartz single grains of each of three sediment samples, following Ou *et al*. (2015). Utilizing the LDAC program (Liang & Forman, 2019) and the DRAC program (Durcan *et al*., 2015) plus the Minimum Age model (Galbraith *et al*., 1999) to calculate minimum ages, practically the same dates were obtained using either program. The DRAC results yielded ages of: 114.4 ± 20.2 ka for LF 3; 170.7 ± 40.0 ka for LF 2; and 56.1 ± 13.5 ka for LF 1. The equivalent dose (De) of two samples: LF 3 and LF 2 are 218.6 ± 36.1 Gy and 332.2 ± 75.1 Gy, respectively, which exceed saturated dose of quartz (~200 Gy). Nevertheless, these two cases are stratigraphically consistent and young upwards, and we can state confidently that the ages exceed 100ka. Sample LF 1 yielded an equivalent dose of 152.1 ± 35.5 Gy, which indicates that the sample is not saturated and the age is dependable.

Assuming a simple 'layer-cake' stratigraphy pertains for the fill within the sinkhole, the OSL date for LF 1 is not in chronostratigraphic order. However, sequential sedimentation within a cone-shaped hollow that has no base is likely not so simplistic. A sediment deposit that partially fills a bedrock walled cone, can be subject to collapse directly over the underlying sinkhole, resulting in debris evacuation downwards leaving a marginal deposit attached to the cone walls. Thus, the stratigraphic sequencing of dates can be explained by a sequence of sediment infills as illustrated in Figure 7. In this model, LF 2 is deposited first before being capped by LF 3, and then both lithofacies were subject to basal collapse before LF 1 was emplaced, plugging the space between the older units. The whole sequence was then capped by the till (LF 4), remaining in place until the sampled section was produced by the collapse in 2019 (Fig. 4).

Taking a cautious approach to interpretation of the older ages (> 100ka), it is reasonable to ascribe the oldest date to either the end of Marine Isotope Stage (MIS) 6 or more likely the beginning of the Ipswichian interglacial (MIS 5e). Thus, sedimentary fill (LF 2) was first deposited in a pre-existing solutional limestone fissure probably following the coldest phase of MIS 6 (the late Wolstonian glaciation, 180–126 ka; Gibbard & Clark, 2011). The LF 2 fill most likely was due to aeolian and surface water transportation after Wolstonian ice had retreated from the region; similar processes but a change in climate were associated with Ipswichian deposition (sometime around 114ka; MIS 5e), producing the LF 3 deposits which are distinct in colour and lie above LF 2. Collapse of these deposits at an unknown date produced a void, which was then filled, or partially-filled, during the Middle Devensian Substage (MIS 3) by LF 1. No alluvial deposits attributed to MIS 2 occur in the sinkhole. Rather, the sequence was capped by a thin till, which is undated but is likely of late MIS 2 age (*cf*., Livingstone *et al*., 2008, 2012), when northward flowing Eden Valley ice sealed the sinkhole and its sedimentary fill. Given the dynamic nature of ice flow events in the region during the last glaciation (Evans *et al*. 2009; Livingstone *et al*. 2012), it is likely that subglacial processes partially modified (deformed and/or partially cannibalised) the top of the sinkhole fill and any earlier (Devensian) tills prior to the emplacement of LF 4 but, nevertheless, Ipswichian deposits clearly survived the last glaciation.

*Sinkhole evolution model*

As will be evident from the description of the sedimentary section above, the collapse resulted in the loss of the central portion of a stratified sandy infill that had filled the depression above the sinkhole. A compact till caps the sandy infill and is preserved as a sloping eroded surface a few metres wide around the margins of the sinkhole. Elsewhere, the sloping surface is an undifferentiated mix of till and the sandy infill. This unvegetated and unstable surface slopes towards the centre of the sinkhole, where vertical sections of the intact till lie conformably over glacially or periglacially deformed sands (Fig. 7).

During late MIS 6 or early MIS 5e, surface washed or blown sands disappeared down into the karstic drainage system until such time as an obstruction at depth plugged it. Subsequently, LF 2 accumulated above the blockage (Fig. 7A) and then unit LF 3 during MIS 5e (Fig. 7B). Collapse of the fill occurred before MIS 3 (Fig. 7C), following which a new obstruction caused sediment fill LF 1 to accumulate during MIS 3 (Fig. 7D). During the Dimlington Stadial, glacial ice covered the region and ice flow would have stripped all or much of the regolith, leaving the prior deposited sediment deep in the fissures. Till then was deposited over the sedimentary fill, infilling any depression and leaving no surface expression of the sinkhole (Fig. 7E).

Initial collapse of the LF 2/3 sedimentary fill above the sinkhole most likely occurred due to percolation of surface water drainage dislodging a blockage at the base of the sinkhole, as occurred again in 2019. Changes in the level of the water table such that air or water might occur below the fill, coupled with dissolution and/or mechanical failure of the limestone may also have contributed to the dislodgement of the fill. Nonetheless, the slumped infill was washed down the karst drainage system (Fig. 7F) to leave a distinct conical depression and section as was revealed in 2019.

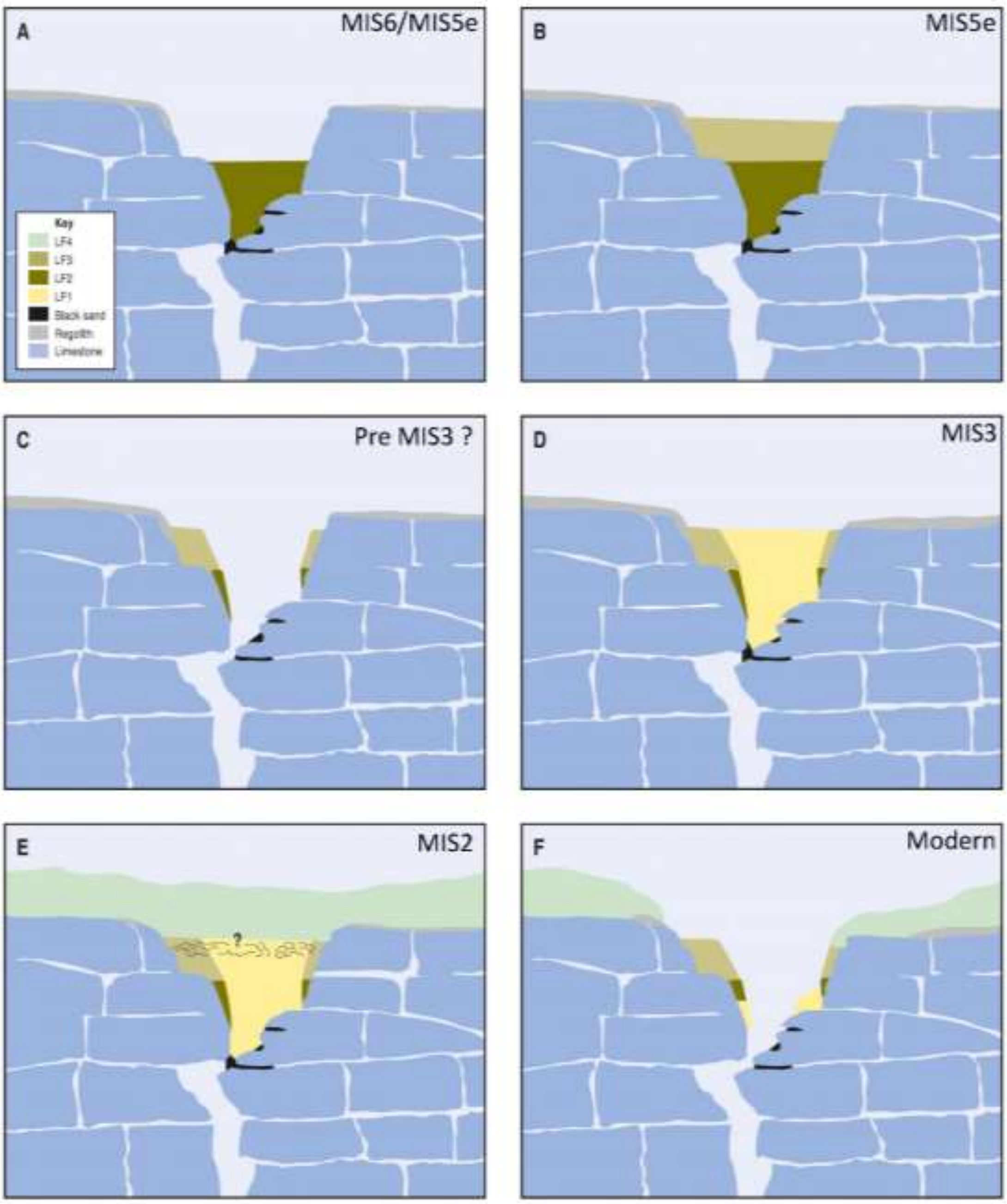


*Figure 7: Diagrammatic representation of sinkhole development: A) Base of an initially open dissolution sinkhole becomes clogged with in-washed fine sediments (LF 2 – MIS 6? Or early MIS 5e) derived from surface regolith and old, weathered glacigenic deposits due to surface water drainage; B) In-washed fine sediments (LF 3 – MIS 5e) due to surface water drainage, cap the deposits below; C) Collapse of infill deposits occurs due to percolation of surface water drainage dislodging the blockage at the base of the sinkhole. The infill is lost down the karst drainage system. Residual masses of the infill deposits (LF 2/3) are preserved on the flanks of the sinkhole; D) Blockage is re-established and in-wash of fines (LF 1 – MIS 3) fills the central portion of the sinkhole (the vertical extent of LF 1 is unknown but depicted here to extend upwards through both LFs 2 and 3); E) Late Devensian till (LF 4 – MIS 2) is emplaced over the*

*alluvial fill, with a deformation (shear) zone forming a glacitectonite at the base of the till (the architecture of this boundary is unknown due to its later removal by collapse of the sinkhole fill); F) Collapse of deposits in 2019.*

**Discussion**

There has been a long debate as to the age of formation of karst features in northern England (e.g. Sweeting 1972; Goldie 1996, 2006) with larger examples, such as dolines (100's m scale), being regarded as pre-Devensian (Goldie, 2006; Waltham, 2013). In contrast, Goldie (2006) and Marker & Goldie (2007) noted that the smaller sinkholes (10's m scale) might be attributed to post-glacial (MIS 1) dissolution. However, sinkholes containing residual diamicton fill (and occasional large erratics – assumed to relate to MIS 2) are common in the region. In cases where the diamicton fill is thin, to support the assertion of Goldie (2006) and Marker & Goldie (2007), it could be argued that the diamicton originally formed a horizontal blanket above limestone terrain to be redistributed by slumping into the evolving sinkhole as dissolution promoted deepening in the post-glacial period. Large erratics would have been lowered into sinkholes by slumping at the same time. However, it is also possible that the diamicton, including large erratics, was trapped in sinkholes as basal ice crossed the pre-existing sinkholes during glaciation (the Dimlington Stadial; MIS 2). Where the diamicton deposits are thick within sinkholes there is a clear suspicion that the initial development of many (if not all) of the larger sinkholes predates the Dimlington Stadial and is related to karst processes in interstadials (Marker & Goldie, 2007), most likely intervals within MIS 5, which assertion is confirmed by the present study. Thus, the limestone surface at Askham Common was a lapiés (karren; Sweeting, 1972) karst surface before the Dimlington Stadial.

Our sinkhole fill is capped by till, so Holocene local surface weathering and development of soil can be excluded as the source of the sandy units beneath the till, as the OSL dates confirm. The present study strongly supports the notion that karst surfaces in northern England developed before the Late Devensian (Goldie, 1996, 2006) as dissolution, due to surface runoff percolating down through the jointed limestone, opened joints forming a sub-surface drainage system linking joints and opened bedding planes at least as early as MIS 5e, if not late in MIS 6; an older initiation of fissuring is also possible. Locally some joints will have widened sufficiently at the ground surface to allow conical depressions to occur in any overlying sediment to form sinkholes well before the Devensian Stage. In other cases, where surface deposits are absent, joint widening would result in small, yet distinct, water sinks (runnel holes; Goldie, 1996) where fissures widened, but these surfaces lack the distinctive cone-shaped depressions of sinkholes. In either case, copious water flow is required (Ford & Williams, 1988) to dissolve the limestone, which usually cannot be supplied under the modern hydrological regimen (Goldie, 1996), and which might point to wetter and warmer sub-stages within MIS 5. Yet, periglacial snow melt or paraglacial ice melt (permafrost degradation) could have supplied the water (Goldie, 1996; cf. Ford 1984, 1987) during or after cooler sub-stages. In periglacial conditions wind-blown sediment would be a source of loess and coarser cover sands.

McCormac (2003) noted that bare limestone pavements of the region lack sinkholes, whereas pavements covered by glacial diamicton often feature dropout sinkholes or suffusion dolines (Sweeting, 1972; Ford, 1979; Veress, 2016), which suggests a relationship between sinkholes and glaciation. Within the western Pennine hills, bare limestone pavement usually is found at higher elevations (>300m), with Dimlington Stadial till limited to altitudes below 300m. The possible association of till with sinkholes might indicate that pre-Dimlington Stadial limestone fissures and sinkholes were accentuated by glacial meltwater in active drainage points for polythermal or warmed-based ice at lower altitudes. Indeed, pre-existing subterranean cave networks have been proposed as significant controls on meltwater drainage routes (*e.g*., Ford, 1979, 1983, 1987; Lauritzen, 1984, 1986; Murphy *et al*., 2001; Farrant *et al*., 2013; Telbisz, 2019). In contrast, cold-based ice at higher elevations likely was associated with little or no subglacial meltwater production, as is evident in the widespread development of diagnostic cold-based ice indicators such as lateral meltwater channels on upper valley slopes (*cf*., Dyke 1993; Greenwood *et al*. 2007; Livingstone *et al*. 2010; Evans *et al*., 2018; Evans & Young, 2022).

The points made in the previous paragraph highlight an unresolved issue: the relative role of dissolution due to runoff during warmer sub-stages and the role of subglacial meltwater. In this context, it is useful to consider how a karst surface would develop or even be destroyed during the Dimlington Stadial ice cover. In numerical models of dissolution of karst conduits consisting of bedding planes punctuated by vertical joints (*viz* Fig. 7), the rate of water flow is the primary control on the evolution of conduit patterns, with the initial network geometry providing a secondary control (Jiang *et al*., 2022). The role of the network geometry assumes increased significance if the thin limestone beds are mechanically incompetent and then are subject to localised subglacial plucking, which can be facilitated by injection of till and/or ice into fractures and the concomitant jacking of rock fragments (Rea & Whalley 1994; Evans *et al*. 1998; Evans 2018; Hall *et al*. 2020). The sediment infill and its apparent pre-Devensian age suggest that the karst network locally was not expanded by subglacial meltwater nor was it significantly altered by plucking. Instead, the infilled vertical fissures were sealed by till, uncoupling the karst and subglacial drainage systems.

The fine tails to the size distributions of sedimentary units LF 1, LF 2 and LF 3 are interpreted as representing local loess generated during ice-free periods from as early as late MIS 6, but more probably MIS 5e. Loess is reported widely in the region on Carboniferous basement rocks (Wilson, 2008) of the north Pennines (Vincent & Lee, 1981; 1982) as well as further south (Marker & Goldie, 2007) but, in contrast to the present results, usually is post-MIS 2 in origin. Many of these latter deposits are blown sand of Holocene age (Vincent *et al*., 2011) although Telfer *et al*. (2009) have reported deglacial ages (*c.,* 19–16 ka) as well as ages (*c.,* 27 ka) potentially pre-dating the LGM ice extent in northwest England. The latter, together with the results presented here, indicate that loess, cover sands and diamictons may have survived beneath ice cover in isolated pockets such as sinkholes throughout the last glacial stadial and earlier cold and warm sub-stages.

**Conclusions**

The sediment fill within a sinkhole formed beneath Late Devensian till on a limestone pavement in northern England consists of three distinct units of alluvium, each due to surface runoff and aeolian deposition. A first phase of alluviation may have occurred during the Wolstonian (MIS 6) but this phase is more securely dated as within the Ipswichian substage (MIS 5e), as is the second phase. A final third phase occurred during MIS 3. The deposits were capped by a Dimlington Stadial (MIS 2) till. The results indicate that substantial solution widened fissures were present in a lapiés (karren) karst surface at the beginning of the Ipswichian substage. Enhanced runoff, greater than that experienced today within sinkholes, may be required to widen solution fissures. Although such increased runoff might be associated with the climate of previous interglacial substages, the exact role of basal glacial meltwater drainage processes, as well as the nature of their interaction with the karstic drainage system, remain unclear.

**Acknowledgements**

Luba Meshkova is thanked for producing Fig. 1.

## Data Availability Statement

Data are available upon request to the first author.

## References

Chiverrell, R.C. & Thomas, G.S.P., 2010. Extent and timing of the last glacial maximum (LGM) in Britain and Ireland: a review. *Journal of Quaternary Science*, 25, 535-549.

Clare, T., Wilkinson, D.M., 2006. Moor Divock revisited: some new sites, survey and interpretations. *Transactions of the Cumberland and Westmorland Antiquarian and Archaeological Society, Series 3*, 6, 1-16.

Clayton, K.M., 1981. Explanatory description of the landforms of the Malham Area. *Field Studies*, 5, 389-423.

Davies, B.J., Livingstone, S.J., Roberts, *et al*., Dynamic ice stream retreat in the central sector of the last British-Irish Ice Sheet. *Quaternary Science Reviews*, 225, 105989.

Durcan, J.A., King, G.E., Duller, G.A.T., 2015. DRAC: Dose Rate and Age Calculator for trapped charge dating. *Quaternary Geochronology*, 28. 54-61.

Dyke, A.S., 1993. Landscapes of cold-centred Late Wisconsinan ice caps, Arctic Canada. *Progress in Physical Geography* 17, 223–247.

Evans, D.J.A. 2018. *Till: A Glacial Process Sedimentology*. Wiley-Blackwell, Chichester.

Evans, D.J.A., Young, B., 2022. The abnormally large “hushes” of Teesdale, North Pennines, England: Differentiating mining legacy and natural landforms in glaciated Carboniferous bedrock terrain. *Proceedings of the Geologists’ Association,* 133, 457-480.

Evans, D.J.A., Dinnage, M., Roberts, D.H., 2018. Glacial geomorphology of Teesdale, northern Pennines, England: Implications for upland styles of ice stream operation and deglaciation in the British-Irish Ice Sheet. *Proceedings of the Geologists' Association,* 129, 697–735.

Evans D.J.A., Livingstone S.J., Vieli A., *et al*., 2009. The palaeoglaciology of the central sector of the British and Irish Ice Sheet: reconciling glacial geomorphology and preliminary ice sheet modelling. *Quaternary Science Reviews* 28, 740-758.

Evans, D. J. A., Rea, B. R., Benn, D. I. 1998. Subglacial deformation and bedrock plucking in areas of hard bedrock. *Glacial Geology and Geomorphology* rp04/1998 (paper available from authors).

Farrant, A.R., Simms, M.J., Noble, S.R., 2013. Subterranean glacial spillways: an example from the karst of South Wales, UK. 16th International Congress of Speleology, Brno, Czech Republic, 21-28 July 2013.

Ford, D.C., 1979. A review of alpine karst in the southern Rocky Mountains of Canada. *National Speleological Society of America Bulletin,* 41, 53-65.

Ford, D.C., 1983. Effects of glaciations upon karst aquifers in Canada. *Journal of Hydrology,* 61, 149–158.

Ford, D.C., 1984. Karst groundwater activity and landform genesis in modern permafrost regions of Canada. In: La Fleur, R.G. (ed.), *Groundwater as a Geomorphic Agent*. Allen & Unwin, London, pp. 340-350.

Ford, D.C., 1987. Effects of glaciations and permafrost upon the development of karst in Canada. *Earth Surface Processes and Landforms,* 12, 507–521.

Ford, D.C., Stanton, W.I., 1968. Geomorphology of the south-central Mendip Hills. *Proceedings of the Geologists' Association* 79, 401-427.

Ford, D. C., Williams, P. W., 1989. *Karst Geomorphology and Hydrology*. Unwin Hyman, London. 601 pp.

Galbraith, R.F., Roberts, R.G., Laslett, G., *et al*., 1999. Optical dating of single and multiple grains of quartz from Jinmium Rock Shelter, northern Australia: part I, experimental design and statistical models. *Archaeometry*, 41, 339-364.

Gibbard, P.L., Clark, C.D., 2011. Chapter 7 - Pleistocene Glaciation Limits in Great Britain. Developments in Quaternary Sciences, 15, 75-93.

Goldie, H.S. 1996. The limestone pavements of Great Asby Scar, Cumbria, UK. *Environmental Geology*, 28, 128-136.

Goldie, H.S., 2006. Mature intermediate-scale surface karst landforms in NW England and their relations to glacial erosion. In A. Kiss and Mezõsi, G. and S. Z. Taj (Eds). Komyezet es tarsadalom (Landscape, Environment and Society. Studies in Honour of Professor Ilona Bárány-kevei on the occasion of her Birthday), Hungary: Szeged. 225-237.

Greenwood, S.L., Clark, C.D., Hughes, A.L.C., 2007. Formalising an inversion methodology for reconstructing ice-sheet retreat patterns from meltwater channels: application to the British Ice Sheet. *Journal of Quaternary Science* 22, 637–645.

Hall, A. M., Krabbendam, M., van Boeckel, M., *et al*., 2020. Glacial ripping: Geomorphological evidence from Sweden for a new process of glacial erosion. *Geografiska Annaler* A102, 333–353.

Hoogsteen, M.J.J., Lantinga, E.A., Bakker, E.J., et al., 2018. An Evaluation of the Loss-on-Ignition Method for Determining the Soil Organic Matter Content of Calcareous Soils. *Communications in Soil Science and Plant Analysis*, 49, 1541-1552, DOI: 10.1080/00103624.2018.1474475

Jennings, J.N., 1975. Doline morphometry as a morphogenetic tool: New Zealand examples. New Zealand Geographer 31, 6–28.

Jiang, C., Wang, X., Pu, S*., et al.,* 2022. Incipient karst generation in jointed layered carbonates: Insights from three-dimensional hydro-chemical simulations. *Journal of Hydrology*, 610, 12783

Lauritzen, S.E., 1984. Evidence of subglacial karstification in Glomdal, Svartisen. *Norsk Geografisk Tidsskrift*, 38, 169–170.

Lauritzen, S.E., 1986. Kvithola at Hauske, northern Norway: an example of ice-contact speleogenesis. *Norsk Geologisk Tidsskrift*, 66, 153–161.

Liang, P., Forman, S. L., 2019. LDAC: An Excel-based program for luminescence equivalent dose and burial age calculations. *Ancient TL*, 37(2), 21-40.

Livingstone S.J., Evans D.J.A., Ó Cofaigh C. *et al*., 2010. The Brampton kame belt and Pennine escarpment meltwater channel system (Cumbria, UK): Morphology, sedimentology and formation. *Proceedings of the Geologists' Association* 121, 423-443.

Livingstone S.J., Ó Cofaigh C. & Evans D.J.A., 2008. Glacial geomorphology of the central sector of the last British-Irish Ice Sheet. *Journal of Maps* 2008, 358-377.

Marker, M.E., Goldie, H. S., 2007. Large karst depressions on the Yorkshire Dales limestone: Interim results and discussion. An early indication of a new paradigm. *Cave and Karst Science*, 34, 117-128.

McCormac, M., 2003. The Upper Palaeozoic rocks and Quaternary deposits of the Shap and Penrith district, Cumbria (part of Sheet 30, England and Wales). *British Geological Survey Report*, RR/01/10, 30pp.

Murphy, P.J., 1999. Sediment studies in Joint Hole, Chapel-le-dale, North Yorkshire., UK. *Cave and Karst Science*, 26, 87-90.

Murphy, P.J., Smallshire, R., Midgley, C. 2001. The sediments of Illusion Pot, Kingsdale, UK: evidence for subglacial utilisation of a karst conduit in the Yorkshire Dales? *Cave and Karst Science* 28, 29-34.

Murray, A.S., Wintle, A.G., 2000. Luminescence dating of quartz using an improved single-aliquot regenerative-dose protocol. *Radiation Measurements*, 32, 57-73.

Ou, X.J., Duller, G.A.T., Roberts, H.M., *et al*., 2015. Single grain optically stimulated luminescence dating of glacial sediments from the Baiyu Valley, southeastern Tibet. *Quaternary Geochronology*, 30: 314-319.

Rea, B. R. and Whalley, W. B. 1994. Subglacial observations from Øksfjordjøkelen, north Norway. *Earth Surface Processes and Landforms* 19, 659–73.

Rose, J., 1985. The Dimlington Stadial/Dimlington Chronozone: a proposal for naming the main glacial episode of the Late Devensian in Britain. *Boreas*, 14, 225-230.

Scourse, J.D., Haapaniemi, A.I., Colmenero-Hidalgo, E., *et al*., 2009. Growth, dynamics and deglaciation of the last British–Irish ice sheet: the deep-sea ice-rafted detritus record. *Quaternary Science Reviews*, 28, 3066–3084.

Sweeting, M.M., 1972. *Karst Landforms*. Macmillan, London.

Telbisz, T., 2019. Characteristics and genesis of subsurface features in glaciokarst terrains. In: Veress, M., Telbisz, T., Tóth, G., Lóczy, D., Ruban, D.A., Gutak, J.M. (Eds.), *Glaciokarsts*. Springer Nature, Switzerland, pp. 221–245.

Telfer, M. W., Wilson, P., Lord, T. C., *et al*., 2009. New constraints on the age of the last ice-sheet glaciation in north-west England using Optically Stimulated Luminescence dating. *Journal of Quaternary Science*, 24, 906–915.

Veress, M. 2016. Postglacial evolution of paleodepressions in glaciokarst areas of the Alps and Dinarides. *Zeitschrift für Geomorphologie*, 60, 343-358.

Veress, M., 2019. Karst landforms of glaciokarst and their development. In: Veress, M., Telbisz, T., Tóth, G., Lóczy, D., Ruban, D.A. & Gutak, J.M. (eds.), Glaciokarsts. Springer Nature, Switzerland, pp. 115-219.

Veress, M., Telbisz, T., Tóth, G., Lóczy, D., Ruban, D.A. & Gutak, J.M. (eds.), 2019. Glaciokarsts. Springer Nature, Switzerland.

Vincent, P., 1985. Quaternary geomorphology of the southern Lake District and Morecambe Bay area. In: Johnson, R.H. (Ed.), The Geomorphology of North-west England. Manchester University Press, Manchester, pp. 158– 177.

Vincent, P. J., Lee, M. P., 1981. Some observations on the loess around Morecambe Bay, North West England. *Proceedings of the Yorkshire Geological Society,* 43, 3, 281-294.

Vincent, P.J., Lee, M.P., 1982. Snow patches on Farleton Fell, South-East Cumbria. *The Geographical Journal*, 148, 337-342.

Vincent, P. J., Lord, T. C., Telfer, M. W., *et al*., 2011. Early Holocene loessic colluviation in northwest England: new evidence for the 8.2 ka event in the terrestrial record? *Boreas*, 40, 105–115. 10.1111/j.1502-3885.2010.00172. x. ISSN 0300-9483.

Waltham, A.C., 2013. Karst geomorphology, pp 65-92 In: Waltham, A.C. & Lowe, D., 2013. Caves and Karst of the Yorkshire Dales, Vol. 1, British cave Research Association, 255pp.

Waltham, A.C., Bell, F.G., Culshaw, M.G., 2005, Sinkholes and Subsidence – Karst and Cavernous Rocks in Engineering and Construction, Springer/Praxis Publishing, Chichester, UK, 382pp.

Waltham, A.C., Fookes, P.G., 2003. Engineering classification of karst ground conditions. *Quarterly Journal of Engineering Geology and Hydrogeology*, 36, 101-118.

Waltham, A.C. & Lowe, D., 2013. Caves and Karst of the Yorkshire Dales, Vol. 1, British Cave Research Association, 255pp.

West, R.G., Gibbard, P.L., Boreham, S. , Rolfe, C. 2014. Geology and geomorphology of the Palaeolithic site at High Lodge, Mildenhall, Suffolk, England. *Proceedings of the Yorkshire Geological Society* 60, 99-121.

Wilson, P., Vincent, P.J., Telfer, M.W., *et al*., 2008. Optically stimulated luminescence (OSL) dating of loessic sediments and cemented scree in northwest England. *The Holocene*, 18, 1101–1112.